Title: TDP-43 proteinopathy alters the ribosome association of multiple mRNAs including the glypican Dally-like protein (Dlp)/GPC6

Authors: Erik M Lehmkuhl[1], Suvithanandhini Loganathan[1], Eric Alsop[2] Alexander D Blythe[1], Tina Kovalik[3], Dianne Barrameda[1], Chuol Kueth[1], Randall J Eck[1] , Bhavani B Siddegowda[1], Archi Joardar[1], Nicholas P Mortimore[1], Robert Bowser[3], Kendall Van Keuren-Jensen[2], and Daniela C Zarnescu[1,4,5]

[1]Department of Cellular and Molecular Biology, University of Arizona, Tucson, AZ, [2]Translational Genomics Research Institute, Phoenix, AZ, [3]Department of Neurobiology, Barrow Neurological Institute, Phoenix, AZ, [4]Department of Neuroscience, University of Arizona, Tucson, AZ, [5]Department of Neurology, University of Arizona, Tucson, AZ

Corresponding Author:

Daniela C Zarnescu, PhD

Department of Cellular and Molecular Biology, University of Arizona

1007 E. Lowell St, LSS RM 548A, Tucson, AZ 857 USA

Tel: 520-626-1478, Email: zarnescu@email.arizona.edu

Keywords:

ALS, TDP-43, translation, motor neuron, neuromuscular junction, glypican, Wnt signaling, Drosophila

Acknowledgements:

We thank members of the Zarnescu lab, including Samantha Macklin. Taylor Wingfield, Rebekah Keating Godfrey, Zachary Hammer. Hannah Ball. Maria Macias, Ernesto Manzo, Matthew

Scandura, Josh Paree, Alyssa Coyne, and Ben Zaepfel for help with dissections and comments on the manuscript. We also thank Herman Dierick, Takeshi Iwatsubo, Paul Taylor and David Morton for providing Drosophila strains. We acknowledge the Bloomington Drosophila Stock Center and the University of Iowa Developmental Studies Hybridoma Bank for supplying reagents. We thank the Barrow Neurological Institute ALS Tissue Bank and Target ALS Postmortem Tissue Core for access to tissues and slides, and all patients for participating in this study. We also thank the New York Genome Center ALS Consortium for providing access to the RNA-seq database. Funding was provided by National Institutes of Health NIH NS091299 RO1, Sandra Harsha Estate (to DCZ), the ARCS foundation and NIH T32-GM008659 (to EML), the Undergraduate Biological Research Program (to ADB), the Beckman Scholars Program (to RJE), the UArizona Graduate College Award (to CK), a Muscular Dystrophy Association B2I award (to AJ), Target ALS Foundation (to RB) and donations on behalf of ALS patients (to KJ).

Abstract:

Amyotrophic lateral sclerosis (ALS) is a genetically heterogeneous neurodegenerative disease in which 97% of patients exhibit cytoplasmic aggregates containing the RNA binding protein TDP-43. Using a combination of RNA immunoprecipitations and tagged ribosome affinity purifications in *Drosophila* models of TDP-43 proteinopathy, we identified several TDP-43 dependent translational alterations including the glypican Dally like protein (Dlp), a wingless (Wg/Wnt) signaling component. Here we show that *dlp* mRNA is enriched in TDP-43 protein complexes and depleted from ribosomes in the context of TDP-43 proteinopathy. We also show that *dlp* mRNA is insolubilized and Dlp protein is significantly depleted from neuromuscular synapses while steady state transcript levels remain unchanged, consistent with mRNA sequestration and translation inhibition. Furthermore, we find that Dlp accumulates in cytoplasmic puncta in the *Drosophila* ventral cord, supporting the possibility of added axonal transport deficits, a well-established ALS phenotype. Notably, overexpression of *dlp* in *Drosophila* motor neurons is sufficient to mitigate TDP-43 dependent neurodegenerative phenotypes indicating that *dlp* is a physiologically relevant target of TDP-43. Finally, we show that similar to Dlp in the *Drosophila* ventral cord, the human ortholog GPC6 forms puncta-like structures in ALS patient spinal cords, further supporting a role for Dlp/GPC6 in TDP-43 induced neurodegeneration.

Introduction:

Amyotrophic lateral sclerosis (ALS) is a neurodegenerative disorder characterized by the progressive loss of motor neuron function, culminating in death due to respiratory failure [27,65]. Mutations in several dozen genes including SOD1 [73], TDP-43 [38,80], and C9orf72 [15,70] have been implicated in disease pathogenesis, however for >79% of patients the cause of disease remains unknown [43] suggesting that yet-to-be-uncovered mechanisms significantly contribute to the majority of ALS cases.

Several cellular processes have been linked to ALS including neuroinflammatory response [52], cellular metabolism [86,18], RNA processing, axonal transport and protein homeostasis [85]. Additionally, in >97% of patient spinal cords, motor neurons exhibit cytoplasmic puncta containing the RNA binding protein TDP-43 (TAR DNA Binding Protein 43) [48,63]. Although only 2-3% of ALS patients possess TDP-43 mutations [38,80,89,63], taken together, these findings suggest a key role for TDP-43 in ALS pathogenesis regardless of etiology.

TDP-43 is a nucleo-cytoplasmic shuttling, DNA/RNA binding protein which is predominantly localized to the nucleus where it regulates transcription [82] and splicing [22,88]. In the cytoplasm, TDP-43 regulates stress granule dynamics [59,17,21,40] as well as axonal and dendritic mRNA localization and translation [1,12,9]. In disease, TDP-43 is depleted from the nucleus, which causes splicing defects, derepression of cryptic exons [46] and increased retrotransposon expression [50,84,42,61]. TDP-43 has been shown to induce toxicity through both nuclear loss- and cytoplasmic gain-of-function mechanisms [92,90,78]. Indeed, when mislocalized to the cytoplasm, TDP-43 associates with a plethora of RNA containing complexes including stress and transport granules [75,91,49] as well as protein complexes devoid of RNA [26,57]. TDP-43 has also been shown to influence the translation of specific mRNAs, both as a negative and as a positive regulator [11,12,55,62,9]. Taken together these findings suggest a complex role for TDP-43 in translation regulation, which may be related to the formation of TDP-

43 cytoplasmic puncta in disease and altered protein expression and/or localization of its mRNA targets.

A potential mechanism by which TDP-43 cytoplasmic inclusions dysregulate translation is by altering the ribosomes' access to mRNAs, as suggested by the previously proposed "ribostasis hypothesis" [69]. Further substantiating this model are recent reports of TDP-43 translational targets including *futsch* and *hsc70-4* mRNAs (in axons) [11,12] and *Rac1* mRNA (in dendrites) [9] all of which were identified through candidate approaches. However, the relationship between TDP-43 associated mRNAs and translation in disease has not yet been studied through an unbiased approach. Here we used a combined RNA immunoprecipitation (RIP) and translating ribosome affinity purification (TRAP) approach to identify mRNAs that satisfy two criteria: 1) are enriched in TDP-43 complexes and thus have the potential to be regulated by TDP-43, and 2) have their ribosomal association altered in the context of *Drosophila* models of TDP-43 proteinopathy, consistent with an effect on translation. These experiments uncovered the *Drosophila* motor neuron translatome and several candidate mRNA targets and pathways dysregulated at the level of translation in the context of TDP-43 proteinopathy *in vivo*.

Among several novel mRNA targets dysregulated by TDP-43 proteinopathy, we identified Dally-like protein (Dlp) as a candidate target of TDP-43 mediated translational inhibition. Dlp is a glypican-type heparan sulfate proteoglycan (HSPG), containing a protein core and attached glycosaminoglycan (GAG) chain that has been described as a regulator of wingless (Wg/Wnt) [95] and Liprin alpha receptor (LAR) mediated signaling at the neuromuscular junction [81]. Here we show that *dlp* mRNA is enriched in TDP-43 complexes and sequestered in insoluble aggregates, consistent with the ribostasis hypothesis. Indeed, we find that Dlp protein is significantly reduced at the neuromuscular junction while steady state levels of *dlp* transcript remain unchanged further supporting the possibility of translation inhibition at synapses. We also find that Dlp accumulates in cytoplasmic puncta in the context of TDP-43 proteinopathy suggesting the presence of axonal transport deficits as well. Genetic interaction experiments

show that *dlp* overexpression mitigates TDP-43 dependent locomotor deficits and increases lifespan in *Drosophila* models of ALS, suggesting that the glypican Dlp mediates aspects of TDP-43 proteinopathy *in vivo*. Lastly, GPC6, a human homolog of Dlp exhibits aggregate-like accumulation in ALS spinal cords, further supporting the notion that altered Dlp/GPC6 expression contributes to motor neuron degeneration.

Materials and Methods:

***Drosophila* genetics**

w^{1118}; UAS-TDP-43^{WT}-YFP and *w^{1118}; UAS-TDP-43^{G298S}-YFP* were previously described [19,20]. *Drosophila* harboring UAS-RpL10 GFP were obtained from Herman Dierick [87]. *w^{1118}; UAS-TDP-43^{WT} UAS-RpL10-GFP/CyO* and *w^{1118}; UAS-RpL10-GFP/CyO; UAS-TDP-43^{G298S}/TM6B* were generated using *w^{1118}; UAS-TDP-43^{WT}* [72] and *w^{1118}; UAS-TDP-43^{G298S}* [36] using standard genetic approaches. These lines were crossed with the D42 GAL4 driver [29] to achieve motor neuron specific expression. For *dlp* overexpression we used *w^{1118}; P{w[+mC]=UAS-dlp.WT}3* (Bloomington Stock #9160) and for RNAi knock-down we used *y[1] v[1]; P{y[+t7.7] v[+t1.8]=TRiP.GLC01658}attP40* (Bloomington Stock #50540). As a control for the RNAi experiments we used *y[1] v[1]; P{y[+t7.7]=CaryP}attP40* (Bloomington Stock #36304). CRISPR TDP-43 models were previously described [7] and provided by David Morton. For Fz2 and LAR overexpression we used *w[*]; P{w[+mC]=UAS-fz2(ECD)-GPI}3* (Bloomington Stock #44221) and *w[*]; P{w[+mC]=UAS-Lar.K}P4B* (Bloomington Stock #9149), respectively. For Fz2 and Lar knockdown we utilized *y[1] sc[*] v[1] sev[21];P{y[+t7.7]v[+t1.8]=TRiP.HMS05675}attP40* (Bloomington Stock #67863) and *y[1] v[1]; P{y[+t7.7] v[+t1.8]=TRiP.HMS02186}attP40* (Bloomington Stock #40938), respectively.

RNA immunoprecipitations (RIP)

100 third instar larvae expressing TDP-43^{WT}-YFP or TDP-43^{G298S}-YFP were collected and flash

frozen in liquid nitrogen. Frozen larvae were homogenized in lysis buffer (100 mM HEPES Buffer pH 8.0, 1% Triton X-100, 200 mM NaCl, 30 mM EDTA, 350 mM Sucrose, 10% Glycerol, 1 mg/mL Heparin, 1 mM DTT, protease inhibitors (Millipore Sigma 11873580001) and RNAsin Plus 400 units/ml (Fischer Scientific PRN2615). Lysates were centrifuged at 10,000 x g for 10 minutes and then pre-cleared with magnetic beads (Dynabeads Protein A, Thermofisher Scientific 10001D) for 1 hour at 4°C. Magnetic beads bound to chicken anti-GFP antibody (Life tech A-11122) were added to the supernatant followed by rotation at 4 ºC for 2 hours. Next, beads were washed 3 times with a sugar-rich buffer (100 mM HEPES Buffer pH 8.0, 1% Triton X-100, 200 mM NaCl, 30 mM EDTA, 350 mM Sucrose, 10%, Glycerol, 1 mg/mL Heparin, 1 mM DTT, RNAsin Plus 400 u/ml) and 2 times with a low-density buffer (100 mM HEPES Buffer pH 8.0, 1% Triton X-100, 200 mM NaCl, 30 mM EDTA ,1 mg/mL Heparin, 1 mM DTT, RNAsin Plus 400 units/ml (Fischer Scientific PRN2615) followed by resuspension in Qiagen RLT buffer (Qiagen 79216) with 1% 2-mercaptoethanol (Sigma Aldrich M6250).

Tagged ribosomes affinity purifications (TRAP)

RNA associated with ribosomes was immunoprecipitated using a protocol similar to RIP (see above) except that the genotypes were *w^{1118}; UAS-RpL10-GFP/CyO*, *w^{1118}; UAS-TDP-43^{WT} UAS-RpL10-GFP/CyO* and *w^{1118}; UAS-RpL10-GFP/CyO; UAS-TDP-43^{G298S}/TM6B Hu Tb* and the buffers for the immunoprecipitation of RpL10-GFP also included 100 μg/mL cycloheximide.

RNA Isolation

RNA was isolated from the ventral cord lysates, whole larvae inputs, or immunoprecipitations using a Qiagen RNeasy Mini Kit (Qiagen 74104) with quality and quantity determined by a nanodrop spectrophotometer. For fractionation experiments and dissected ventral nerve cords (VNCs) or neuromuscular junctions (NMJ), RNA was isolated using Trizol (Thermofisher Scientific 15596026).

RNA Seq

Isolated RNA was prepared for RNA sequencing using the SMART-seq v4 Ultra Low Input RNA kit (Takara Bio USA 634888). The Nextera XT DNA Library Prep Kit (Illumina FC-131-1024) was used to tag, clean, and pool the samples with quality assayed by an Agilent 2100 Bioanalyzer. The cDNA libraries were sequenced by the Beijing Genomics Institute using an Illumina HiSeq 4000 .

Bioinformatics

Reads were aligned to the Flybase FB2018_05 genome using MAFFT [71] with differential expression analysis conducted through Deseq2 [53]. In RIP experiments, 9812 and 9954 genes were detected in TDP-43^{WT} and TDP-43^{G298S} complexes, respectively. In TRAP experiments, 9711, 9347, and 9669 genes were detected in RpL10 GFP complexes in the control, TDP-43^{WT}, and TDP-43^{G298S} models, respectively. To identify the “normal” motor neuron translatome we calculated the Log2FoldChange between RpL10 IP and RpL10 VNCs. Next, to identify alterations resulting caused by TDP-43 proteinopathy to the motor neuron translatomes, we subtracted the Log2FoldChange between RpL10 IP and RpL10 VNCs from the Log2FoldChange between TDP-43^{WT} or ^{G298S} RpL10 IP and TDP-43^{WT} or ^{G298S} RpL10 IP VNCs. For comparison, we also normalized RpL10 IPs to RpL10 whole larvae inputs (see Supplemental Figure 1). Gene ontology (GO) analyses were conducted using David 6.8 [35,34].

Fractionations

Fractionations were conducted as previously described [11]. In brief, 25 third instar larvae were homogenized in Trizol (Thermofisher Scientific 15596026). Lysates were then centrifuged at 25,000 x g for 30 minutes. The supernatant became the soluble fraction and the pellet was solubilized in urea buffer (30 mM Tris, 7 M Urea, 2 M Thiourea, 4% CHAPS, 1X Protease Inhibitor

Cocktail (Millipore Sigma 11873580001), 0.5 mM PMSF, RNAsin Plus 400 units/ml (Fischer Scientific PRN2615), pH = 8.5) to generate the urea/insoluble fraction.

Western Blots

Westerns were conducted as previously described [12,13]. Primary antibodies used were rabbit anti-beta actin (1:2,000, Cell Signaling Technologies) and mouse anti-Dlp (Iowa Developmental Studies Hybridoma Bank, 1:20, 13G8, Deposited to the DSHB by Beachy, P.A). Secondary antibodies were IRDye 800CW Goat anti-Mouse 1:10,000 (Licor 926-32210) and IRDye 680RD Goat anti-Rabbit 1:10,000 (Licor 925-68071). Membranes were scanned using an Odyssey 2.1 Scanner (Licor).

Immunofluorescence (*Drosophila* tissues)

Third instar ventral nerve cords were dissected as previously described [12]. Primary antibodies/stains used were 1:5 anti-Dlp (antibody 13G8, developed by Phil Beachy, obtained from the Developmental Studies Hybridoma Bank, created by the NICHD of the NIH and maintained at The University of Iowa, Department of Biology, Iowa City, IA 52242) and 1:200 anti-GFP (Rockland 600-102-215). DNA was visualized using Hoechst (1:10,000, Invitrogen H3570). Goat anti-mouse Alexa 568 (1:500 Thermofisher Scientific A-11004) was used as secondary antibody. Samples were imaged using a Zeiss LSM 880 inverted confocal microscope with a 40X oil lens. The size of Dlp puncta was quantified using CellProfiler 3.1.9 [60], with puncta defined as between 6 and 10 pixels. Third instar larval NMJs were dissected as previously described [19,20]. Primary antibodies used were 1:5 anti-Dlp, 1:100 anti-HRP Alexa 647 (Jackson Immuno-research 123-605-021). Goat anti-mouse Alexa Fluor 568 (1:500 Thermofisher Scientific A-11004) was used as secondary antibody. Samples were imaged using a Zeiss LSM 880 NLO upright confocal microscope with a 40X oil lens. Dlp intensity per area was quantified with NIH

imageJ v1.52p within four terminal boutons defined by HRP staining. All images were blinded prior to being analyzed.

Immunohistochemistry (human post-mortem spinal cords)

Post-mortem spinal cord tissue sections were obtained from the Barrow Neurological Institute ALS Tissue Bank and Target ALS Postmortem Tissue Core. All tissue samples were collected after informed consent from the subjects or by the subjects' next of kin, complying with all relevant ethical regulations and approved by the appropriate Institutional Review Boards. Clinical neuropathological diagnoses were made by board certified neuropathologists according to consensus criteria. Subject demographics are listed in Supplemental Table S6. A total of 12 ALS and 4 controls (4 non-neurologic disease controls) were used in this study. Tissue sections were processed and imaged as previously described [3]. All ALS cases contained TDP-43 pathology while the non-neurologic disease controls lack TDP-43 pathology. All sections were stained for GPC6 protein using rabbit polyclonal primary antibody at 1:300 (Bioss bs-2177R). A biotinylated goat anti-rabbit IgG (H+L) was used as secondary antibody (Vector Laboratories, BA-1000, 1:200). Images were blinded, then motor neurons were outlined and inverted in NIH ImageJ, which was also used to quantify GPC6 protein intensity relative to background. CellProfiler 3.1.9 [60], was used to quantify GPC6 puncta, defined between 3 to 13 pixels in diameter.

qRT-PCR

All cDNA was synthesized using Fisher First Strand cDNA synthesis reagents (Thermofisher Scientific K1641). qPCR reactions were conducted using Taqman Fast Advanced Master Mix (Thermofisher Scientific 4444556) and conducted on either an ABI 7100 or Analytik Jena 844-00504-4 qTOWER qPCR machine. *dlp* mRNA was quantified using Taqman assay (Thermofisher Scientific Dm01798597_m1*)* using *GPDH* (Thermofisher Scientific Dm01841185_m1) for normalization. Fold change was calculated using the standard ΔΔCT method [67].

Locomotor assays

Third instar wandering larvae were placed on a grape juice agar plate. After being given 1 minute to acclimate, the larvae were turned on the ventral side and timed until they uprighted themselves and began the first forward motion [12].

Lifespan assays

Freshly emerged males and females (40 per genotype) were isolated and transferred into fresh vials every week. Surviving adults were counted daily. Graphs and statistical analyses were generated in GraphPad Prism 7.0b.

Fluorescent In Situ Hybridization (FISH)

FISH was performed using RNAscope (ACD Bio). A custom probe for dm-dlp and a control probe dm-Gapdh1 were used to detect *dlp* and *Gapdh1* in dissected VNC and NMJs as previously described [93]. Signals were detected using a Zeiss LSM 880 inverted confocal microscope with a 40X oil lens.

Statistical Analyses

For RNA seq analyses, significance was determined using the P adjusted value calculation embedded within Deseq2. All other statistical analyses were performed using GraphPad Prism 7.0. All data shown are mean ± standard error of the mean.

Results:

TDP-43 proteinopathy induces a broad range of translational changes in motor neurons

TDP-43 has been shown to associate with a plethora of RNA targets and regulate various aspects of RNA processing including RNA localization and translation [1,12,62]. These findings suggest

that cytoplasmic TDP-43, which is a hallmark of disease, has multiple opportunities to cause alterations in the motor neuron proteome and contribute to pathogenesis. To uncover some of these alterations, we set out to define TDP-43 dependent changes in the motor neuron translatome *in vivo* using *Drosophila* models of TDP-43 proteinopathy that recapitulate key aspects of the disease including locomotor defects, cytoplasmic aggregates and reduced lifespan [20,19]. We hypothesized that while some of translational alterations may be an indirect consequence of neurodegeneration, others are directly caused by TDP-43, possibly through mRNA association with, and sequestration into, TDP-43 cytoplasmic complexes. To distinguish between direct versus indirect effects on the translatome we set out to identify mRNAs that are both enriched with TDP-43 and translationally dysregulated in motor neurons *in vivo* using a combination of RNA immunoprecipitations (RIP) and Translating Ribosomes Affinity Purifications (TRAP) [87,31] in *Drosophila* models of TDP-43 proteinopathy. To this end, we first used third instar larvae expressing human TDP-43 protein specifically in motor neurons via the GAL4-UAS system (D42 GAL4 > UAS-TDP-43-YFP) and performed immunoprecipitation experiments to pull down TDP-43 and associated mRNAs (RIP). The mRNAs associated with TDP-43 (WT or mutant G298S) were isolated and subjected to RNA sequencing (see Materials and Methods, and Figure 1a). Bioinformatic analyses identified several mRNAs significantly enriched with TDP-43, as determined by comparing TDP-43 associated mRNAs from the whole larvae immunoprecipitations with the transcriptome of dissected ventral nerve cords expressing the appropriate TDP-43 variant (TDP-43 WT or mutant G298S, see Figures 1b,c). Notably, these analyses identified a previously published TDP-43 mRNA target, *futsch* [12] to be enriched with TDP-43 in our data set (TDP-43^{WT}, Log2FC = 2.44, Padj = 8.07E-37; TDP-43^{G298S}, Log2FC = 2.68, Padj = 6.86E-12) and also several novel TDP-43 associated RNAs. While 1,892 mRNAs were shared by both TDP-43 variants (Log2FC>2, Padj <0.05), approximately 25% of mRNAs enriched with TDP-43 were unique to TDP-43^{WT} or TDP-43^{G298S} (2,554 total mRNAs enriched with TDP-43 WT and 2,508 total mRNAs enriched with TDP-43 G298S, see Figure 1d) . This

substantiates previous evidence that wild-type and mutant TDP-43 variants cause toxicity in part through distinct mechanisms [11]. In addition, we found that out of 834 TDP-43 interacting mRNAs recently identified in mammalian neurons using TRIBE (targets of RNA-binding proteins identified by editing) [32] about 1/3 were enriched in our *Drosophila* RIP data sets (Supplemental Table S1).

Next, to identify the *in vivo* motor neuron translatome and alterations induced by TDP-43 proteinopathy (see Materials and Methods, and Figure 1e) we conducted TRAP experiments [87,31]. To this end, RpL10-GFP was expressed in motor neurons using D42 GAL4 either on its own, or together with TDP-43^{WT} or TDP-43^{G298S}. Following ribosome immunoprecipitations we isolated total RNA and conducted RNA seq, detecting ~9500 mRNAs (9,711 mRNAs for RpL10 controls, 9,347 for TDP-43 WT and 9,669 for TDP-43 G298S, see Materials and Methods). Subsequent comparisons of the mRNAs enriched with ribosomes precipitated from larvae expressing RpL10-GFP, RpL10-GFP TDP-43^{WT} or RpL10-GFP TDP-43^{G298S} in motor neurons with the transcriptomes of dissected ventral nerve cords of the appropriate genotype (RpL10-GFP, RpL10-GFP TDP-43^{WT} or RpL10 GFP TDP-43^{G298S}) identified genes enriched with, or depleted from, motor neurons ribosomes in both in the RpL10-GFP control and the ALS models relative to the dissected VNC transcriptome (Figures 1f,g,h, and Supplemental Figure 1S). Further bioinformatic analyses using DAVID [35,34] identified pathways enriched in the “normal” motor neuron translatome (*i.e.*, RpL10-GFP control) including “oxidation reduction process” (P_{value} = 5.16E-17) among others. Additionally, “neurogenesis” was depleted in the control motor neuron translatome (P_{value} = 2.18E-20), as expected, given that we conducted the experiment in post-mitotic motor neurons (see Table 1 and Supplemental Tables S2-4).).

In addition, these analyses identified several pathways with altered ribosome association in the *Drosophila* models of TDP-43 proteinopathy relative to the RpL10 control, including cytoplasmic translation and energy metabolism that were previously associated with ALS [69,14,86] (Tables 1 and Supplemental Tables S2-4). Notably, we detected increased association

with ribosomes for *CG6762*, the *Drosophila* ortholog of human SRXN1, (TDP-43^{WT}, Log2FC = 0.673, Padj = 2.79E-32; TDP-43^{G298S}, Log2FC = 0.328, Padj = 2.50E-51), one of 14 genes that exhibited increased translation in a human cell model of TDP-43^{A315T} proteinopathy [62].

dally-like protein (_dlp_) mRNA, a glypican involved in wingless (Wg/Wnt) signaling is sequestered in insoluble complexes in _Drosophila_ models of TDP-43 proteinopathy

To uncover top functional pathways enriched in the "normal" motor neuron translatome we next used String, which is based on known physical and genetic interactions [83]. These analyses highlighted an enrichment in Wg/Wnt signaling genes (Figure 2a); the top 5% of genes translated in motor neurons contain 61% more Wg/Wnt signaling genes than would be present by random selection, suggesting an important role for Wg/Wnt signaling in motor neuron maintenance and function. Interestingly, amongst Wg/Wnt pathway genes, *dlp* mRNA was identified as a candidate target of TDP-43 mediated translational inhibition due to enrichment with TDP-43 complexes (TDP-43^{WT}, Log2FC = 3.62, Padj = 8.32E-57; TDP-43^{G298S}, Log2FC = 4.63, Padj = 2.47E-57) and a slight, albeit statistically significant depletion from ribosomes in the context of TDP-43 proteinopathy (TDP-43^{WT}, Log2FC = -1.03, Padj = 0.027; TDP-43^{G298S}, Log2FC = -0.85, Padj = 0.012), see also Supplemental Table S5. *dlp* encodes a glypican, a member of the heparin sulfate proteoglycan (HSPG) family, expressed on the plasma membrane via a GPI anchor or secreted in the extracellular matrix. HSPGs consist of a protein core and several heparan sulfate (HS) glycosaminoglycan (GAG) linear polysaccharide chains which exhibit complex sulfation patterns that dictate the ability of the HSPGs to interact with ligands such as *wingless* [95]. In *Drosophila*, Dlp was shown to function as a co-factor and competitive inhibitor for binding to the Wg/Wnt pathway receptor Frizzled2 [95] and also to regulate the activity of the phosphatase LAR at the neuromuscular junction [81,37] (Figure 2b). Given the dual regulatory role of Dlp in Wg/Wnt signaling, it is difficult to predict how alterations in *dlp* expression would affect Wg/Wnt targets.

We did however find that both TDP-43^{WT} and TDP-43^{G298S} resulted in decreased *frizzled2* mRNA association with ribosomes (TDP-43^{WT}, Log2FC= -1.00, Padj. =0.026; TDP-43^{G298S}, Log2FC= -0.56, Padj. = 0.027), suggesting that Frizzled2 expression is reduced, which according to previous studies causes increased Wg/Wnt signaling [4]. Counter to this scenario, both TDP-43^{WT} and TDP-43^{G298S} showed increased association with ribosomes for *ovo/shavenbaby* mRNA (TDP-43^{WT}, Log2FC = 2.74, P Value = 4.38E-8; TDP-43^{G298S}, Log2FC = 3.02, P Value = 2.15E-21) whose expression is negatively regulated by Wg/Wnt signaling [66]. Further studies are needed to determine the relationship between TDP-43 and Wg/Wnt signaling in the context of TDP-43 proteinopathy. Lastly, GPI-anchored Dlp protein is frequently cleaved, which modifies its interactions with Frizzled2 receptor [41], further suggesting a complex relationship between Dlp and Wg/Wnt signaling.

To validate *dlp* mRNA's association with TDP-43 we first performed TDP-43 immunoprecipitations from whole larvae expressing either TDP-43^{WT} or TDP-43^{G298S} then isolated the associated RNA and used RT-qPCR to amplify *dlp* mRNA. These experiments showed that indeed, *dlp* mRNA was enriched with both TDP-43^{WT} (Log2FC = 6.11, P_{value} = 0.005) and TDP-43^{G298S} (Log2FC = 6.46, P_{value} = 2.82E-5) relative to the whole larval input (Figure 2c), confirming the RIP mRNA seq data (Figure 1a-d).

Next, to determine whether *dlp* mRNA is insolubilized as predicted by the ribostasis hypothesis, we conducted subcellular fractionations and quantified *dlp* mRNA in the soluble and insoluble/urea fractions from third instar larvae expressing TDP-43 in motor neurons. These experiments showed that *dlp* mRNA is significantly insolubilized in the context of TDP-43^{G298S} (Fold change = 2.35, P_{value} = 0.050, Figure 2d) but not in the context of TDP-43^{WT}, suggesting that *dlp* mRNA is sequestered in insoluble complexes in a variant dependent manner. Further substantiating this finding, *dlp* mRNA was insolubilized in a TDP-43^{G294A} (Fold change = 2.51, P_{value} = 0.034, Figure 2e) but not in the TDP-43^{WT} CRISPR fly model of ALS in which the endogenous *Drosophila* TBPH gene has been replaced with human TDP-43 [7]. Taken together

these results indicate that *dlp* mRNA is a novel TDP-43 candidate target that associates with insoluble aggregates in the context of TDP-43 proteinopathy and suggest that Wg/Wnt signaling may be altered in disease.

Dlp protein levels are altered in the neuromuscular system in the context of TDP-43 proteinopathy

A possible outcome of *dlp* mRNA enrichment with TDP-43 complexes, insolubilization and decreased association with ribosomes is inhibition of Dlp protein synthesis. To test the impact of TDP-43 proteinopathy on Dlp protein expression we conducted immunofluorescence experiments in the larval neuromuscular system. We first examined Dlp expression in the ventral nerve cord (VNC), which comprises motor neuron cell bodies and neurites, [24] and at the neuromuscular junction (NMJ) [39] (Figure 3). While no major changes in Dlp expression were detected in the motor neuron somatic cytoplasm (data not shown), striking aggregate-like structures were observed in the neuropil when either TDP-43 WT or mutant G298S were overexpressed (see Figures 3a-g). Quantification of Dlp granularity with CellProfiler (see Materials and Methods) shows that both TDP-43^{WT} or TDP-43^{G298S} proteinopathy cause a statistically significant increase in Dlp granule size (TDP-43^{WT}, Fold Change = 2.35, P_{value} = 0.008; TDP-43^{G298S}, Fold Change = 2.43, P_{value} = 0.009; Figure 3g). Further substantiating this result are findings that Dlp protein is significantly increased in TDP-43^{G298S} VNCs, as indicated by western blotting experiments (Supplemental Figure S3a).

In contrast to the VNCs, there was a visible reduction in Dlp expression at the larval NMJ. Quantification of Dlp protein levels within synaptic boutons at the NMJs shows a trend downwards for TDP-43^{WT} and a statistically significant decrease for TDP-43^{G298S} compared to w^{1118} controls (TDP-43^{WT}, decreased 20.1%, P_{value} = 0.21; TDP-43^{G298S}, decreased 40.8%, P_{value} = 0.014, Figures 3h-n). These results indicate that TDP-43 proteinopathy causes altered Dlp protein expression, more specifically a reduction at synaptic terminals and aggregate like structures in the VNC

neuropil. To investigate whether these alterations are post-transcriptional, as suggested by the RIP and TRAP experiments, we used fluorescence in situ hybridization (RNAScope) to examine *dlp* mRNA localization in the VNC and at the NMJ. Since we were not able to detect a specific signal, possibly due to low levels of expression (data not shown) we performed RT-qPCR experiments using dissected VNCs and larval NMJ preparations and found no significant changes in *dlp* mRNA levels between TDP-43 proteinopathy models and controls (Supplemental Figure S3c-d). Although the VNC and NMJ qPCR samples contain multiple cell types, which could reduce our ability to detect mRNA differences caused by TDP-43 overexpression specifically in motor neurons, collectively, these experiments suggest that Dlp expression is regulated by TDP-43 post-transcriptionally likely through a combination of translation and axonal trafficking.

dlp is a modifier of TDP-43 dependent locomotor deficits and lifespan in _Drosophila_ models of proteinopathy

Next, to test whether *dlp* mRNA is an effector of TDP-43 proteinopathy, we overexpressed *dlp* using the motor neuron specific driver D42 GAL4 on its own and in the context of TDP-43^{WT} or TDP-43^{G298S} and measured its effect on TDP-43 induced locomotor defects. Using larval turning assays to measure locomotor function we found that although *dlp* overexpression (*dlp* OE) on its own resulted in a higher turning time (15.3 +/- 1.01 seconds, P_{Value} = 2E-6 compared to w^{1118} controls 8.95 +/- 0.46 seconds), in the context of either TDP-43^{WT} or TDP-43^{G298S} disease models, it caused a lower turning time, indicating a rescue of locomotor dysfunction (11.30 +/- 0.56 seconds, P_{Value} = 0.041 compared to 13.40 +/- 0.69 seconds for TDP-43^{WT} alone; 12.50 +/- 0.83 seconds, P_{Value} = 6.4E-3 compared to 16.40 +/- 1.16 seconds for TDP-43^{G298S} alone, see Figure 4a). Consistent with these results, *dlp* knockdown by RNA interference (RNAi), which also caused higher larval turning times on its own (17.5 +/- 0.76 seconds, P_{value} = 1.4E-5 compared to 8.64 +/- 0.45 seconds for attp40 controls) enhanced locomotor deficits in both ALS models based on TDP-43 (16.9 +/- 1.21 seconds, P_{value} = 0.037 compared to 14.00 +/- 0.76 seconds for TDP-43^{WT} alone;

TDP-43^{G298S} 29.30 +/- 2.56 seconds , P_{value} = 1.8E-4 compared to 16.10 +/- 0.73 seconds for TDP-43^{G298S} alone, see Figure 4b).

Additionally, overexpression of *dlp* was sufficient to increase lifespan in the context of TDP-43^{WT} (average 52.6 days, P_{value} = 0.017 compared to 44.7 days for TDP-43^{WT} alone, see Figure 4c). Surprisingly, *dlp* overexpression on its own was also sufficient to extend lifespan (average 77.8 days, P_{value} = 3.29E-6 compared to 65.3 days for w^{1118} controls, see Figure 4c). We were not able to determine the effect of *dlp* OE on lifespan in the TDP-43^{G298S} model due to synthetic pupal lethality. Overall, these experiments indicate that precise *dlp* expression levels are critical for locomotor function and lifespan and restoring *dlp* levels by overexpression is beneficial in the context of TDP-43 proteinopathy.

The expression of GPC6, a Dlp ortholog is altered in patient spinal cords

To validate our findings from *Drosophila* in human patient derived tissues, we evaluated the expression and sub-cellular distribution of the Dlp human ortholog GPC6 [33] in lumbar spinal cord from ALS patients compared to non-neurological controls using immunohistochemistry. These experiments showed that GPC6 appears increased and more granular in ALS spinal cords compared to controls (Figure 5, for patient demographic information see Supplemental Table S6). Quantification of staining intensity and granularity showed that indeed, GPC6 protein levels were increased (Fold Change = 4.03, P_{value}=0.001, see Figure 5c) and more aggregate-like GPC6 puncta were present in ALS patient motor neurons compared to controls (Fold Change = 7.03, P_{value} = 0.015). Interestingly, this increased granular appearance of GPC6 in ALS spinal cords resembles the Dlp protein levels and localization observed in the *Drosophila* VNCs expressing TDP-43^{G298S} (Figure 3). To further investigate the presence of GPC6 alterations in patient tissues, we analyzed the New York Genome Center ALS Consortium data RNA-seq data set (provided by Target ALS) and found that across 116 sALS and 31 control spinal cords *GPC6* mRNA was

increased in sALS samples (Log2FC = 0.46, Padj = 0.023), consistent with increased GPC6 protein levels we observed in ALS spinal cords compared to controls. Additionally, ZNRF3-AS1, an antisense RNA that modifies expression of the Wg/Wnt regulator ZNRF3 [30], exhibits increased expression in patient spinal tissue (Log2FC = 4.30, Padj = 3.57E-4) further suggesting that Wg/Wnt signaling is dysregulated in ALS pathogenesis. Together, these findings show that GPC6 protein alterations in patient tissues resemble those identified in the *Drosophila* models of TDP-43 proteinopathy and suggest that glypican function may also be altered at neuromuscular synapses in ALS, consistent with a recent report of GPC4/6 reduction in SOD1 mice [5].

Discussion:

TDP-43 proteinopathy is a hallmark of ALS [48,64] and has been observed in several other neurodegenerative diseases [48,8,45,58,76], yet the contribution of TDP-43 proteinopathy to neurodegeneration remains poorly understood. TDP-43 contributes to multiple steps on RNA processing from splicing to translational regulation providing multiple opportunities for gene expression dysregulation in disease [25,68]. Furthermore, TDP-43 associates with several cytoplasmic complexes including translational machinery [23,74,77,13] and stress granules [10,49,16,59], suggesting a role for TDP-43 in translation inhibition, as predicted by the ribostasis hypothesis [69]. Several specific mRNA targets of TDP-43 mediated translational inhibition have been reported [12,11,55,56]. Among these, when overexpressed, *futsch/MAP1B* and *Hsc70-4/HSPA8* modify disease phenotypes highlighting their contribution to disease [12,11]. Recently, puromycin incorporation experiments in SH-SY5Y neuroblastoma cells showed that increased cytoplasmic TDP-43 reduces global translation through interactions with RACK1 on polyribosomes [74]. In contrast, polysome fractionation experiments in a human cell model showed that ALS associated mutant TDP-43^{A315T} acts as a positive regulator of translation for a subset of specific mRNAs (*e.g.*, Camta1, Mig12, and Dennd4A) [62]. Taken together these

findings highlight a complex and yet-to-be understood function of TDP-43 in translational regulation with evidence supporting roles both as a translational activator and inhibitor.

Here, using a *Drosophila* model of TDP-43 proteinopathy that recapitulates key features of the human disease including locomotor dysfunction and reduced lifespan [19,20] we identified TDP-43 dependent changes in the motor neuron translatome. These experiments identified both pathways previously associated with ALS (*e.g.*, translation, mitochondrial function [6,79]) and novel targets of TDP-43 mediated translational inhibition including the Wg/Wnt signaling regulator *dlp*. It is interesting that cytoplasmic translation is a pathway under-represented in the "normal" motor neuron translatome, yet it is upregulated in the context of TDP-43 proteinopathy. This could reflect a compensatory mechanism whereby degenerating neurons upregulate global translation in response to increased cellular stress or a compensatory mechanism to mitigate cytoplasmic TDP-43's inhibitory effect on translation [74].

In addition to identifying motor neuron specific alterations to the translatome induced by TDP-43 proteinopathy, we identified *dlp* as a direct target of TDP-43 mediated translation inhibition. *dlp* is translated into a membrane bound glypican which modifies LAR activity, thereby modifying transport to the neuromuscular junction [81,37]. Dlp also interacts with the Wg/Wnt pathway receptor Frizzled2, serving as both a co-factor and competitive inhibitor for substrate binding [95]. Genetic manipulation (either overexpression or RNAi knockdown) of both LAR and Frizzled2 resulted in lethality prior to the third instar stage in the context of both TDP-43^{WT} and TDP-43^{G298S} disease models (data not shown). These findings suggest that Dlp is likely an effector of TDP-43 proteinopathy by acting in both of these pathways and are consistent with our TRAP data indicating that the translation of several Wg/Wnt target genes was altered. Discerning how *dlp* alterations affect the motor neuron is further complicated by Dlp's established interactions with the hedgehog [94] and hippo [2] pathways, which will be the focus of future studies.

We show that although TDP-43^{WT} and TDP-43^{G298S} both associate with *dlp* mRNA, and correlate with *dlp* depletion from ribosomes, the severity of some phenotypic alterations was

variant dependent. While overexpression of *dlp* mRNA was sufficient to rescue locomotor dysfunction in the context of both TDP-43 variants, a significant depletion at the neuromuscular junction was observed only in the TDP-43^{G298S} model. Differential results have previously been observed between the TDP-43^{WT} and TDP-43^{G298S} models [11], which are likely the result of increased TDP-43^{G298S} stability [47] and granule viscosity relative to TDP-43^{WT} [28].

In the TDP-43^{G298S} model, analyses of the whole VNC, which contains motor neuron soma and neurites, show that Dlp protein is increased whereas staining at the NMJ revealed a significant reduction in Dlp protein. These findings suggest that TDP-43 dependent translational inhibition is local, which can explain the relatively small depletion of *dlp* mRNA from ribosomes using TRAP, an approach that reflects translational changes in the entire motor neuron rather than specific compartments. It is possible that the synapse specific alteration in Dlp levels could also result from transport deficits, trapping NMJ-bound *dlp* mRNA/Dlp protein in the soma or neurites. Although our qPCR data show no change in *dlp* mRNA levels, we cannot eliminate the possibility of mRNA and/or protein transport defects leading to the accumulation of Dlp in the VNC and reduction at the NMJ. Collectively, our findings suggest a model in which the mislocalization of Dlp we found in flies and patient spinal cords results from a combination of axonal transport and translation inhibition as previously detected for Futsch/MAP1b [12] (see Figure 6 for model). Although more experiments are needed to determine the nature and composition of Dlp puncta we found in the VNC, we speculate that they may reflect the accumulation of endomembrane compartments that were previously shown to be altered in the context of TDP-43 proteinopathy [51].

Our findings that GPC6, a Dlp ortholog is increased in ALS spinal cord motor neurons reveals a striking resemblance to the Dlp granules observed in the *Drosophila* VNC, further highlighting the power of the fly models to predict pathological changes in disease. Interestingly, the formation of heparin sulfate proteoglycan containing puncta has previously been observed in other neurodegenerative disease including Alzheimer's, Parkinson's and SOD1 mediated ALS

(reviewed in [54]) however this has not been previously reported in the context of TDP-43 proteinopathy, nor has a mechanism been proposed. More recently, genetic knockdown of heparan sulfate-modifying enzyme *hse-5* in C. elegans mitigated TDP-43 induced deficits in synaptic transmission [44], further suggesting a link between TDP-43 pathology, neurodegeneration and heparan sulfate proteoglycans such as Dlp/GPC6.

In summary, we report novel translational consequences of TDP-43 proteinopathy and identify the glypican *dlp* as a target of TDP-43 dependent proteinopathy, which suggests multiple therapeutic strategies including restoration of axonal transport, synaptic specific protein expression as well as Wg/Wnt and other related Dlp signaling pathways in ALS.

References:

1. Alami NH, Smith RB, Carrasco MA, Williams LA, Winborn CS, Han SS, et al. (2014) Axonal transport of TDP-43 mRNA granules is impaired by ALS-causing mutations. Neuron 81:536-543. doi:10.1016/j.neuron.2013.12.018
2. Baena-Lopez LA, Rodriguez I, Baonza A (2008) The tumor suppressor genes dachsous and fat modulate different signalling pathways by regulating dally and dally-like. Proc Natl Acad Sci U S A 105:9645-9650. doi:10.1073/pnas.0803747105
3. Bakkar N, Kovalik T, Lorenzini I, Spangler S, Lacoste A, Sponaugle K, et al. (2018) Artificial intelligence in neurodegenerative disease research: use of IBM Watson to identify additional RNA-binding proteins altered in amyotrophic lateral sclerosis. Acta Neuropathol 135:227-247. doi:10.1007/s00401-017-1785-8
4. Cadigan KM, Fish MP, Rulifson EJ, Nusse R (1998) Wingless repression of Drosophila frizzled 2 expression shapes the Wingless morphogen gradient in the wing. Cell 93:767-777. doi:10.1016/s0092-8674(00)81438-5

5. Cave C, Park S, Rodriguez M, Nakamura M, Hoke A, Pletnikov M, et al (2017) GDE2 is essential for neuronal survival in the postnatal mammalian spinal cord. Mol Neurodegener 12:8. doi:10.1186/s13024-017-0148-1

6. Cestra G, Rossi S, Di Salvio M, Cozzolino M (2017) Control of mRNA Translation in ALS Proteinopathy. Front Mol Neurosci 10:85. doi:10.3389/fnmol.2017.00085

7. Chang JC, Morton DB (2017) Drosophila lines with mutant and wild type human TDP-43 replacing the endogenous gene reveals phosphorylation and ubiquitination in mutant lines in the absence of viability or lifespan defects. PLoS One 12:e0180828. doi:10.1371/journal.pone.0180828

8. Chang XL, Tan MS, Tan L, Yu JT (2016) The Role of TDP-43 in Alzheimer's Disease. Mol Neurobiol 53:3349-3359. doi:10.1007/s12035-015-9264-5

9. Chu JF, Majumder P, Chatterjee B, Huang SL, Shen CJ (2019) TDP-43 Regulates Coupled Dendritic mRNA Transport-Translation Processes in Co-operation with FMRP and Staufen1. Cell Rep 29:3118-3133 e3116. doi:10.1016/j.celrep.2019.10.061

10. Colombrita C, Zennaro E, Fallini C, Weber M, Sommacal A, Buratti E, et al.(2009) TDP-43 is recruited to stress granules in conditions of oxidative insult. J Neurochem 111:1051-1061. doi:10.1111/j.1471-4159.2009.06383.x

11. Coyne AN, Lorenzini I, Chou CC, Torvund M, Rogers RS, Starr A, et al. (2017) Post-transcriptional Inhibition of Hsc70-4/HSPA8 Expression Leads to Synaptic Vesicle Cycling Defects in Multiple Models of ALS. Cell Rep 21:110-125. doi:10.1016/j.celrep.2017.09.028

12. Coyne AN, Siddegowda BB, Estes PS, Johannesmeyer J, Kovalik T, Daniel SG, et al. (2014) Futsch/MAP1B mRNA Is a Translational Target of TDP-43 and Is Neuroprotective in a Drosophila Model of Amyotrophic Lateral Sclerosis. J Neurosci 34:15962-15974. doi:10.1523/JNEUROSCI.2526-14.2014

13. Coyne AN, Yamada SB, Siddegowda BB, Estes PS, Zaepfel BL, Johannesmeyer JS, et al. (2015) Fragile X protein mitigates TDP-43 toxicity by remodeling RNA granules and restoring translation. Hum Mol Genet 24:6886-6898. doi:10.1093/hmg/ddv389
14. Coyne AN, Zaepfel BL, Zarnescu DC (2017) Failure to Deliver and Translate-New Insights into RNA Dysregulation in ALS. Frontiers in cellular neuroscience 11:243. doi:10.3389/fncel.2017.00243
15. DeJesus-Hernandez M, Mackenzie IR, Boeve BF, Boxer AL, Baker M, Rutherford NJ, et al. (2011) Expanded GGGGCC hexanucleotide repeat in noncoding region of C9ORF72 causes chromosome 9p-linked FTD and ALS. Neuron 72:245-256. doi:10.1016/j.neuron.2011.09.011
16. Dewey CM, Cenik B, Sephton CF, Dries DR, Mayer P, Good SK, et al. (2011) TDP-43 is directed to stress granules by sorbitol, a novel physiological osmotic and oxidative stressor. Mol Cell Biol 31:1098-1108. doi:10.1128/MCB.01279-10
17. Dewey CM, Cenik B, Sephton CF, Johnson BA, Herz J, Yu G (2012) TDP-43 aggregation in neurodegeneration: are stress granules the key? Brain Res 1462:16-25. doi:10.1016/j.brainres.2012.02.032
18. Dupuis L, Pradat PF, Ludolph AC, Loeffler JP (2011) Energy metabolism in amyotrophic lateral sclerosis. Lancet Neurol 10:75-82. doi:10.1016/S1474-4422(10)70224-6
19. Estes PS, Boehringer A, Zwick R, Tang JE, Grigsby B, Zarnescu DC (2011) Wild-type and A315T mutant TDP-43 exert differential neurotoxicity in a Drosophila model of ALS. Human molecular genetics 20:2308-2321. doi:10.1093/hmg/ddr124
20. Estes PS, Daniel SG, McCallum AP, Boehringer AV, Sukhina AS, Zwick RA, et al. (2013) Motor neurons and glia exhibit specific individualized responses to TDP-43 expression in a Drosophila model of amyotrophic lateral sclerosis. Disease models & mechanisms 6:721-733. doi:10.1242/dmm.010710

21. Fernandes N, Eshleman N, Buchan JR (2018) Stress Granules and ALS: A Case of Causation or Correlation? Adv Neurobiol 20:173-212. doi:10.1007/978-3-319-89689-2_7
22. Fiesel FC, Weber SS, Supper J, Zell A, Kahle PJ (2012) TDP-43 regulates global translational yield by splicing of exon junction complex component SKAR. Nucleic Acids Res 40:2668-2682. doi:10.1093/nar/gkr1082
23. Freibaum BD, Chitta RK, High AA, Taylor JP (2010) Global analysis of TDP-43 interacting proteins reveals strong association with RNA splicing and translation machinery. J Proteome Res 9:1104-1120. doi:10.1021/pr901076y
24. Gan G, Lv H, Xie W (2014) Morphological identification and development of neurite in Drosophila ventral nerve cord neuropil. PLoS One 9:e105497. doi:10.1371/journal.pone.0105497
25. Gao J, Wang L, Huntley ML, Perry G, Wang X (2018) Pathomechanisms of TDP-43 in neurodegeneration. J Neurochem. doi:10.1111/jnc.14327
26. Gasset-Rosa F, Lu S, Yu H, Chen C, Melamed Z, Guo L, et al. (2019) Cytoplasmic TDP-43 De-mixing Independent of Stress Granules Drives Inhibition of Nuclear Import, Loss of Nuclear TDP-43, and Cell Death. Neuron 102:339-357 e337. doi:10.1016/j.neuron.2019.02.038
27. Gil J, Funalot B, Verschueren A, Danel-Brunaud V, Camu W, Vandenberghe N, et al. (2008) Causes of death amongst French patients with amyotrophic lateral sclerosis: a prospective study. Eur J Neurol 15:1245-1251. doi:10.1111/j.1468-1331.2008.02307.x
28. Gopal PP, Nirschl JJ, Klinman E, Holzbaur EL (2017) Amyotrophic lateral sclerosis-linked mutations increase the viscosity of liquid-like TDP-43 RNP granules in neurons. Proc Natl Acad Sci U S A 114:E2466-E2475. doi:10.1073/pnas.1614462114
29. Gustafson K, Boulianne GL (1996) Distinct expression patterns detected within individual tissues by the GAL4 enhancer trap technique. Genome 39:174-182

30. Hao HX, Xie Y, Zhang Y, Charlat O, Oster E, Avello M, et al. (2012) ZNRF3 promotes Wnt receptor turnover in an R-spondin-sensitive manner. Nature 485:195-200. doi:10.1038/nature11019
31. Heiman M, Schaefer A, Gong S, Peterson JD, Day M, Ramsey KE, et al. (2008) A translational profiling approach for the molecular characterization of CNS cell types. Cell 135:738-748. doi:10.1016/j.cell.2008.10.028
32. Herzog JJ, Xu W, Deshpande M, Rahman R, Suib H, Rodal AA, et al. (2020) TDP-43 dysfunction restricts dendritic complexity by inhibiting CREB activation and altering gene expression. Proc Natl Acad Sci U S A 117:11760-11769. doi:10.1073/pnas.1917038117
33. Hu Y, Flockhart I, Vinayagam A, Bergwitz C, Berger B, Perrimon N, et al.(2011) An integrative approach to ortholog prediction for disease-focused and other functional studies. BMC Bioinformatics 12:357. doi:10.1186/1471-2105-12-357
34. Huang da W, Sherman BT, Lempicki RA (2009) Bioinformatics enrichment tools: paths toward the comprehensive functional analysis of large gene lists. Nucleic Acids Res 37:1-13. doi:10.1093/nar/gkn923
35. Huang da W, Sherman BT, Lempicki RA (2009) Systematic and integrative analysis of large gene lists using DAVID bioinformatics resources. Nat Protoc 4:44-57. doi:10.1038/nprot.2008.211
36. Ihara R, Matsukawa K, Nagata Y, Kunugi H, Tsuji S, Chihara T, et al. (2013) RNA binding mediates neurotoxicity in the transgenic Drosophila model of TDP-43 proteinopathy. Human molecular genetics 22:4474-4484. doi:10.1093/hmg/ddt296
37. Johnson KG, Tenney AP, Ghose A, Duckworth AM, Higashi ME, Parfitt K, et al. (2006) The HSPGs Syndecan and Dallylike bind the receptor phosphatase LAR and exert distinct effects on synaptic development. Neuron 49:517-531. doi:10.1016/j.neuron.2006.01.026

38. Kabashi E, Valdmanis PN, Dion P, Spiegelman D, McConkey BJ, Vande Velde C, et al. (2008) TARDBP mutations in individuals with sporadic and familial amyotrophic lateral sclerosis. Nat Genet 40:572-574
39. Keshishian H, Broadie K, Chiba A, Bate M (1996) The drosophila neuromuscular junction: a model system for studying synaptic development and function. Annu Rev Neurosci 19:545-575. doi:10.1146/annurev.ne.19.030196.002553
40. Khalfallah Y, Kuta R, Grasmuck C, Prat A, Durham HD, Vande Velde C (2018) TDP-43 regulation of stress granule dynamics in neurodegenerative disease-relevant cell types. Sci Rep 8:7551. doi:10.1038/s41598-018-25767-0
41. Kreuger J, Perez L, Giraldez AJ, Cohen SM (2004) Opposing activities of Dally-like glypican at high and low levels of Wingless morphogen activity. Dev Cell 7:503-512. doi:10.1016/j.devcel.2004.08.005
42. Krug L, Chatterjee N, Borges-Monroy R, Hearn S, Liao WW, Morrill K, et al. (2017) Retrotransposon activation contributes to neurodegeneration in a Drosophila TDP-43 model of ALS. PLoS Genet 13:e1006635. doi:10.1371/journal.pgen.1006635
43. Lattante S, Ciura S, Rouleau GA, Kabashi E (2015) Defining the genetic connection linking amyotrophic lateral sclerosis (ALS) with frontotemporal dementia (FTD). Trends Genet 31:263-273. doi:10.1016/j.tig.2015.03.005
44. Liachko NF, Saxton AD, McMillan PJ, Strovas TJ, Keene CD, Bird TD, et al. (2019) Genome wide analysis reveals heparan sulfate epimerase modulates TDP-43 proteinopathy. PLoS Genet 15:e1008526. doi:10.1371/journal.pgen.1008526
45. Ling H, Hardy J, Zetterberg H (2015) Neurological consequences of traumatic brain injuries in sports. Mol Cell Neurosci 66:114-122. doi:10.1016/j.mcn.2015.03.012
46. Ling JP, Pletnikova O, Troncoso JC, Wong PC (2015) TDP-43 repression of nonconserved cryptic exons is compromised in ALS-FTD. Science 349:650-655. doi:10.1126/science.aab0983

47. Ling SC, Albuquerque CP, Han JS, Lagier-Tourenne C, Tokunaga S, Zhou H, et al (2010) ALS-associated mutations in TDP-43 increase its stability and promote TDP-43 complexes with FUS/TLS. Proc Natl Acad Sci U S A 107:13318-13323. doi:10.1073/pnas.1008227107
48. Ling SC, Polymenidou M, Cleveland DW (2013) Converging mechanisms in ALS and FTD: disrupted RNA and protein homeostasis. Neuron 79:416-438. doi:10.1016/j.neuron.2013.07.033
49. Liu-Yesucevitz L, Bilgutay A, Zhang YJ, Vanderweyde T, Citro A, Mehta T, et al. (2010) Tar DNA binding protein-43 (TDP-43) associates with stress granules: analysis of cultured cells and pathological brain tissue. PLoS One 5:e13250. doi:10.1371/journal.pone.0013250
50. Liu EY, Russ J, Cali CP, Phan JM, Amlie-Wolf A, Lee EB (2019) Loss of Nuclear TDP-43 Is Associated with Decondensation of LINE Retrotransposons. Cell Rep 27:1409-1421 e1406. doi:10.1016/j.celrep.2019.04.003
51. Liu G, Coyne AN, Pei F, Vaughan S, Chaung M, Zarnescu DC, et al. (2017) Endocytosis regulates TDP-43 toxicity and turnover. Nature communications 8:2092. doi:10.1038/s41467-017-02017-x
52. Liu J, Wang F (2017) Role of Neuroinflammation in Amyotrophic Lateral Sclerosis: Cellular Mechanisms and Therapeutic Implications. Front Immunol 8:1005. doi:10.3389/fimmu.2017.01005
53. Love MI, Huber W, Anders S (2014) Moderated estimation of fold change and dispersion for RNA-seq data with DESeq2. Genome Biol 15:550. doi:10.1186/s13059-014-0550-8
54. Maiza A, Chantepie S, Vera C, Fifre A, Huynh MB, Stettler O, et al. (2018) The role of heparan sulfates in protein aggregation and their potential impact on neurodegeneration. FEBS Lett 592:3806-3818. doi:10.1002/1873-3468.13082
55. Majumder P, Chen YT, Bose JK, Wu CC, Cheng WC, Cheng SJ, et al. (2012) TDP-43 regulates the mammalian spinogenesis through translational repression of Rac1. Acta Neuropathol 124:231-245. doi:10.1007/s00401-012-1006-4

56. Majumder P, Chu JF, Chatterjee B, Swamy KB, Shen CJ (2016) Co-regulation of mRNA translation by TDP-43 and Fragile X Syndrome protein FMRP. Acta Neuropathol 132:721-738. doi:10.1007/s00401-016-1603-8
57. Mann JR, Gleixner AM, Mauna JC, Gomes E, DeChellis-Marks MR, Needham PG, et al. (2019) RNA Binding Antagonizes Neurotoxic Phase Transitions of TDP-43. Neuron 102:321-338 e328. doi:10.1016/j.neuron.2019.01.048
58. Markopoulou K, Dickson DW, McComb RD, Wszolek ZK, Katechalidou L, Avery L, et al. (2008) Clinical, neuropathological and genotypic variability in SNCA A53T familial Parkinson's disease. Variability in familial Parkinson's disease. Acta Neuropathol 116:25-35. doi:10.1007/s00401-008-0372-4
59. McDonald KK, Aulas A, Destroismaisons L, Pickles S, Beleac E, Camu W, et al. (2011) TAR DNA-binding protein 43 (TDP-43) regulates stress granule dynamics via differential regulation of G3BP and TIA-1. Hum Mol Genet 20:1400-1410. doi:10.1093/hmg/ddr021
60. McQuin C, Goodman A, Chernyshev V, Kamentsky L, Cimini BA, Karhohs KW, et al.(2018) CellProfiler 3.0: Next-generation image processing for biology. PLoS Biol 16:e2005970. doi:10.1371/journal.pbio.2005970
61. Morera AA, Ahmed NS, Schwartz JC (2019) TDP-43 regulates transcription at protein-coding genes and Alu retrotransposons. Biochim Biophys Acta Gene Regul Mech 1862:194434. doi:10.1016/j.bbagrm.2019.194434
62. Neelagandan N, Gonnella G, Dang S, Janiesch PC, Miller KK, Kuchler K, et al. (2019) TDP-43 enhances translation of specific mRNAs linked to neurodegenerative disease. Nucleic Acids Res 47:341-361. doi:10.1093/nar/gky972
63. Neumann M (2009) Molecular Neuropathology of TDP-43 Proteinopathies. Int J Mol Sci 10:232-246

64. Neumann M, Sampathu DM, Kwong LK, Truax AC, Micsenyi MC, Chou TT, et al. (2006) Ubiquitinated TDP-43 in frontotemporal lobar degeneration and amyotrophic lateral sclerosis. Science 314:130-133
65. Niedermeyer S, Murn M, Choi PJ (2019) Respiratory Failure in Amyotrophic Lateral Sclerosis. Chest 155:401-408. doi:10.1016/j.chest.2018.06.035
66. Payre F, Vincent A, Carreno S (1999) ovo/svb integrates Wingless and DER pathways to control epidermis differentiation. Nature 400:271-275. doi:10.1038/22330
67. Pfaffl MW (2001) A new mathematical model for relative quantification in real-time RT-PCR. Nucleic acids research 29:e45
68. Prasad A, Bharathi V, Sivalingam V, Girdhar A, Patel BK (2019) Molecular Mechanisms of TDP-43 Misfolding and Pathology in Amyotrophic Lateral Sclerosis. Front Mol Neurosci 12:25. doi:10.3389/fnmol.2019.00025
69. Ramaswami M, Taylor JP, Parker R (2013) Altered ribostasis: RNA-protein granules in degenerative disorders. Cell 154:727-736. doi:10.1016/j.cell.2013.07.038
70. Renton AE, Majounie E, Waite A, Simon-Sanchez J, Rollinson S, Gibbs JR, et al. (2011) A hexanucleotide repeat expansion in C9ORF72 is the cause of chromosome 9p21-linked ALS-FTD. Neuron 72:257-268. doi:10.1016/j.neuron.2011.09.010
71. Rio DC, Ares M, Jr., Hannon GJ, Nilsen TW (2010) Purification of RNA using TRIzol (TRI reagent). Cold Spring Harb Protoc 2010:pdb prot5439. doi:10.1101/pdb.prot5439
72. Ritson GP, Custer SK, Freibaum BD, Guinto JB, Geffel D, Moore J, et al. (2010) TDP-43 mediates degeneration in a novel Drosophila model of disease caused by mutations in VCP/p97. J Neurosci 30:7729-7739
73. Rosen DR, Siddique T, Patterson D, Figlewicz DA, Sapp P, Hentati A, et al. (1993) Mutations in Cu/Zn superoxide dismutase gene are associated with familial amyotrophic lateral sclerosis. Nature 362:59-62. doi:10.1038/362059a0

74. Russo A, Scardigli R, La Regina F, Murray ME, Romano N, Dickson DW, et al.(2017) Increased cytoplasmic TDP-43 reduces global protein synthesis by interacting with RACK1 on polyribosomes. Hum Mol Genet 26:1407-1418. doi:10.1093/hmg/ddx035

75. Salajegheh M, Pinkus JL, Taylor JP, Amato AA, Nazareno R, Baloh RH, et al. (2009) Sarcoplasmic redistribution of nuclear TDP-43 in inclusion body myositis. Muscle Nerve 40:19-31

76. Schwab C, Arai T, Hasegawa M, Yu S, McGeer PL (2008) Colocalization of transactivation-responsive DNA-binding protein 43 and huntingtin in inclusions of Huntington disease. J Neuropathol Exp Neurol 67:1159-1165. doi:10.1097/NEN.0b013e31818e8951

77. Sephton CF, Cenik C, Kucukural A, Dammer EB, Cenik B, Han Y, et al. (2011) Identification of Neuronal

RNA Targets of TDP-43-containing Ribonucleoprotein Complexes. J Biol Chem 286:1204-1215. doi:M110.190884 [pii]

78. Shenouda M, Zhang AB, Weichert A, Robertson J (2018) Mechanisms Associated with TDP-43 Neurotoxicity in ALS/FTLD. Adv Neurobiol 20:239-263. doi:10.1007/978-3-319-89689-2_9

79. Smith EF, Shaw PJ, De Vos KJ (2019) The role of mitochondria in amyotrophic lateral sclerosis. Neurosci Lett 710:132933. doi:10.1016/j.neulet.2017.06.052

80. Sreedharan J, Blair IP, Tripathi VB, Hu X, Vance C, Rogelj B, et al. (2008) TDP-43 mutations in familial and sporadic amyotrophic lateral sclerosis. Science 319:1668-1672

81. Stryker E, Johnson KG (2007) LAR, liprin alpha and the regulation of active zone morphogenesis. J Cell Sci 120:3723-3728. doi:10.1242/jcs.03491

82. Swain A, Misulovin Z, Pherson M, Gause M, Mihindukulasuriya K, Rickels RA, et al.(2016) Drosophila TDP-43 RNA-Binding Protein Facilitates Association of Sister Chromatid Cohesion Proteins with Genes, Enhancers and Polycomb Response Elements. PLoS Genet 12:e1006331. doi:10.1371/journal.pgen.1006331

83. Szklarczyk D, Gable AL, Lyon D, Junge A, Wyder S, Huerta-Cepas J, et al. (2019) STRING v11: protein-protein association networks with increased coverage, supporting functional discovery in genome-wide experimental datasets. Nucleic Acids Res 47:D607-D613. doi:10.1093/nar/gky1131
84. Tam OH, Rozhkov NV, Shaw R, Kim D, Hubbard I, Fennessey S, (2019) Postmortem Cortex Samples Identify Distinct Molecular Subtypes of ALS: Retrotransposon Activation, Oxidative Stress, and Activated Glia. Cell Rep 29:1164-1177 e1165. doi:10.1016/j.celrep.2019.09.066
85. Taylor JP, Brown RH, Jr., Cleveland DW (2016) Decoding ALS: from genes to mechanism. Nature 539:197-206. doi:10.1038/nature20413
86. Tefera TW, Borges K (2016) Metabolic Dysfunctions in Amyotrophic Lateral Sclerosis Pathogenesis and Potential Metabolic Treatments. Front Neurosci 10:611. doi:10.3389/fnins.2016.00611
87. Thomas A, Lee PJ, Dalton JE, Nomie KJ, Stoica L, Costa-Mattioli M, et al. (2012) A versatile method for cell-specific profiling of translated mRNAs in Drosophila. PLoS One 7:e40276. doi:10.1371/journal.pone.0040276
88. Tollervey JR, Curk T, Rogelj B, Briese M, Cereda M, Kayikci M, et al. (2011) Characterizing the RNA targets and position-dependent splicing regulation by TDP-43. Nature neuroscience 14:452-458. doi:10.1038/nn.2778
89. Van Deerlin VM, Leverenz JB, Bekris LM, Bird TD, Yuan W, Elman LB, et al. (2008) TARDBP mutations in amyotrophic lateral sclerosis with TDP-43 neuropathology: a genetic and histopathological analysis. Lancet Neurol 7:409-416
90. Vanden Broeck L, Callaerts P, Dermaut B (2014) TDP-43-mediated neurodegeneration: towards a loss-of-function hypothesis? Trends Mol Med 20:66-71. doi:10.1016/j.molmed.2013.11.003

91. Vogler TO, Wheeler JR, Nguyen ED, Hughes MP, Britson KA, Lester E, et al. (2018) TDP-43 and RNA form amyloid-like myo-granules in regenerating muscle. Nature 563:508-513. doi:10.1038/s41586-018-0665-2

92. Walker AK, Spiller KJ, Ge G, Zheng A, Xu Y, Zhou M, et al. (2015) Functional recovery in new mouse models of ALS/FTLD after clearance of pathological cytoplasmic TDP-43. Acta Neuropathol 130:643-660. doi:10.1007/s00401-015-1460-x

93. Wang F, Flanagan J, Su N, Wang LC, Bui S, Nielson A, et al. (2012) RNAscope: a novel in situ RNA analysis platform for formalin-fixed, paraffin-embedded tissues. J Mol Diagn 14:22-29. doi:10.1016/j.jmoldx.2011.08.002

94. Williams EH, Pappano WN, Saunders AM, Kim MS, Leahy DJ, Beachy PA (2010) Dally-like core protein and its mammalian homologues mediate stimulatory and inhibitory effects on Hedgehog signal response. Proc Natl Acad Sci U S A 107:5869-5874. doi:10.1073/pnas.1001777107

95. Yan D, Wu Y, Feng Y, Lin SC, Lin X (2009) The core protein of glypican Dally-like determines its biphasic activity in wingless morphogen signaling. Dev Cell 17:470-481. doi:10.1016/j.devcel.2009.09.001

Tables:

Table 1. Pathways whose mRNAs are enriched or depleted with motor-neuron specific RpL10-GFP ribosomes. Genes enriched > Log2FC 1 or depleted < -1 Log2FC and with Padj < 0.05 underwent pathway analysis through David 6.8. TRAP RpL10-GFP gene enrichment/depletion was determined by comparing RpL10-GFP associated RNA to the transcriptome of the TRAP RpL10-GFP VNC. TRAP enrichment/depletion in TDP-43^{WT} and TDP-43^{G298S} ALS models was determined by comparing RpL10-GFP associated RNA within each genotype to the respective VNC, then subtracting out the enrichment/depletion observed in the control to identify alterations to ribosome association induced by TDP-43 proteinopathy.

TRAP RpL10 Enriched		
Biological Process	Gene Count	P_{Value}
oxidation-reduction process	142	5.16E-17
proteolysis	142	2.43E-11
chitin metabolic process	45	4.33E-10
mesoderm development	33	2.87E-09
transmembrane transport	91	1.06E-08
TRAP RpL10 Depleted		
Biological Process	Gene Count	P_{Value}
cytoplasmic translation	67	1.79E-26
mitochondrial translation	57	7.29E-22
mRNA splicing, via spliceosome	101	1.41E-20
neurogenesis	190	2.98E-20
transcription, DNA-templated	123	3.20E-12
TRAP TDP-43^{WT} Enriched		
Biological Process	Gene Count	P_{Value}
cytoplasmic translation	47	2.18E-27
mitochondrial electron transport, NADH to ubiquinone	18	6.74E-11
mitochondrial translation	27	8E-11
translation	74	1.22E-06
proton transport	11	4.5E-06
TRAP TDP-43^{WT} Depleted		

Biological Process	Gene Count	P_{Value}
regulation of GTPase activity	11	0.000369
protein phosphorylation	29	0.000911
intracellular protein transport	15	0.002235
neuromuscular junction development	9	0.003104
axon guidance	21	0.003458
TRAP TDP-43^{G298S} Enriched		
Biological Process	Gene Count	P_{Value}
cytoplasmic translation	45	4.16E-34
ribosomal small subunit assembly	9	8.4E-07
neuropeptide signaling pathway	13	4.79E-06
translation	50	8.96E-06
ATP synthesis coupled proton transport	7	0.000412
TRAP TDP-43^{G298S} Depleted		
Biological Process	Gene Count	P_{Value}
oxidation-reduction process	30	0.003095
dephosphorylation	8	0.011882
RNA processing	6	0.013224
cell division	8	0.022279
meiotic nuclear division	5	0.023023

Figure legends:

Figure 1. Experimental schemes and results of RIP and TRAP experiments in *Drosophila* models of TDP-43 proteinopathy.

(a). Experimental schematic for RNA immunoprecipitations of human TDP-43, specifically from the motor neurons of third instar larvae. **(b,c).** Volcano plot displaying mRNAs enriched with TDP-43 in TDP-43^{WT} **(b)** and TDP-43^{G298S}. All genes associated with TDP-43 (log2FC > 0) are displayed regardless of significance. **(c)** proteinopathy, relative to transcript levels in the ventral nerve cord. **(d).** Venn diagram of mRNAs enriched with TDP-43 in two disease models (Padj <0.05, log2foldchange > 1). **(e).** Experimental schematic for immunoprecipitation of RpL10-GFP specifically from the motor neurons of third instar larvae. **(f,g,h).** Volcano plots displaying RNA enrichment with RpL10 in w^{1118} control third instar larvae **(f)**, or TDP-43^{WT} **(g)**, and TDP-43^{G298S} **(h)** expressing larvae relative to transcript levels in the ventral nerve cord. All genes are displayed regardless of significance.

Figure 2. *dlp* mRNA, a modulator of Wg/Wnt signaling is enriched in TDP-43 complexes and sequestered in insoluble fractions in the context of TDP-43 proteinopathy. (a). STRING diagram [83] depicting relationship between Wg/Wnt signaling genes in the top 10% of the TRAP control IP normalized counts (D42>RpL10 GFP, see Materials and Methods). Line thickness between genes is correlated with the strength of the interaction as defined by STRING. **(b).** Diagram of Wg/Wnt signaling pathway including Dlp. **(c).** qPCR quantification of *dlp* mRNA enrichment with TDP-43 complexes in TDP-43^{WT} and TDP-43^{G298S} expressing larvae (D42>TDP-43 WT or G298S). Enrichment in TDP-43 complexes is shown as arbitrary units (*a.u.*) after normalization to input. **(d, e).** Schematic of fractionation experiments and qPCR quantification of *dlp* mRNA levels in the insoluble fraction (Urea fraction) of TDP-43^{WT} or TDP-43^{G298S} expressing larvae (relative to w^{1118} controls) **(d)**, and CRISPR-TDP-43^{G94A} (relative to CRISPR-TDP-43^{WT}).

Significance was determined using the Kruskall-Wallis Test **(d)** or Student's T Test. **(e).** * = P_{value} < 0.05.

Figure 3. Dlp protein expression is altered by TDP-43 proteinopathy.

(a-c) Representative images of w^{1118}, TDP-43^{WT} and TDP-43^{G298S} VNCs stained for Dlp, DNA and TDP-43. **(d-f)** High magnification images of insets indicated in (a-c) showing Dlp granules in the neuropil (arrows). **(g).** Quantification of Dlp granule size. N =3. **(h).** Quantification of Dlp protein relative to bouton area in terminal boutons. N = 7-10. Significance determined using the Kruskall Wallis test. **(i-k)** Representative images of w^{1118}, TDP-43^{WT} and TDP-43^{G298S} NMJs stained for Dlp and HRP. **(l-n).** High magnification images of insets indicated in **(i-k)**. Genotypes and stainings, as indicated. Scale bars: **(a)**, **(d)** - 45 μm, **(i)**, **(l)** - 20 μm. * = P_{value} < 0.05.

Figure 4. Altered *dlp* mRNA levels modify TDP-43 induced locomotion and lifespan defects. (a). Larval turning times for *dlp* mRNA overexpression in the w^{1118} genetic background (control for OE experiments), TDP-43^{WT}, and TDP-43^{G298S}. **(b).** Larval turning times for *dlp* RNAi in the attp40 genetic background (control for RNAi experiments), TDP-43^{WT}, and TDP-43^{G298S}. For **(a,b)** N = 33-40. Significance determined using the MannU Whitney Test. * = P_{value} < 0.05. **(c).** Quantification of lifespan for TDP-43^{WT} and the w^{1118} control in the context of *dlp* mRNA overexpression and knockdown through RNAi. N =40. Significance determined using the Mantel Cox Test. * = P_{value} < 0.05.

Figure 5. GPC6, a Dlp ortholog exhibits increased expression and altered localization in patient spinal tissues. (a). Representative image of a control spinal cord. N =4. **(b).** Representative image of ALS patient spinal cord. N = 12. **(c)** Quantification of GPC6 intensity and GPC6 granules in post-mortem spinal tissue. Arrowheads indicate motor neurons. Significance determined using MannU Whitney Test. * = P_{value} < 0.05. Scale bar in **(a)** - 40 μm. * = P_{value} < 0.05.

Figure 6. Dlp is altered in the context of TDP-43 proteinopathy. Dlp mRNA is enriched in TDP-43 complexes, depleted from ribosomes and sequestered in insoluble/urea complexes. Taken together, these findings and our observations of Dlp protein being reduced at the NMJ and accumulating in puncta within cell bodies and neuropils suggest multiple cellular defects including local translation inhibition at synapses, axonal trafficking and endomembrane trafficking deficits.

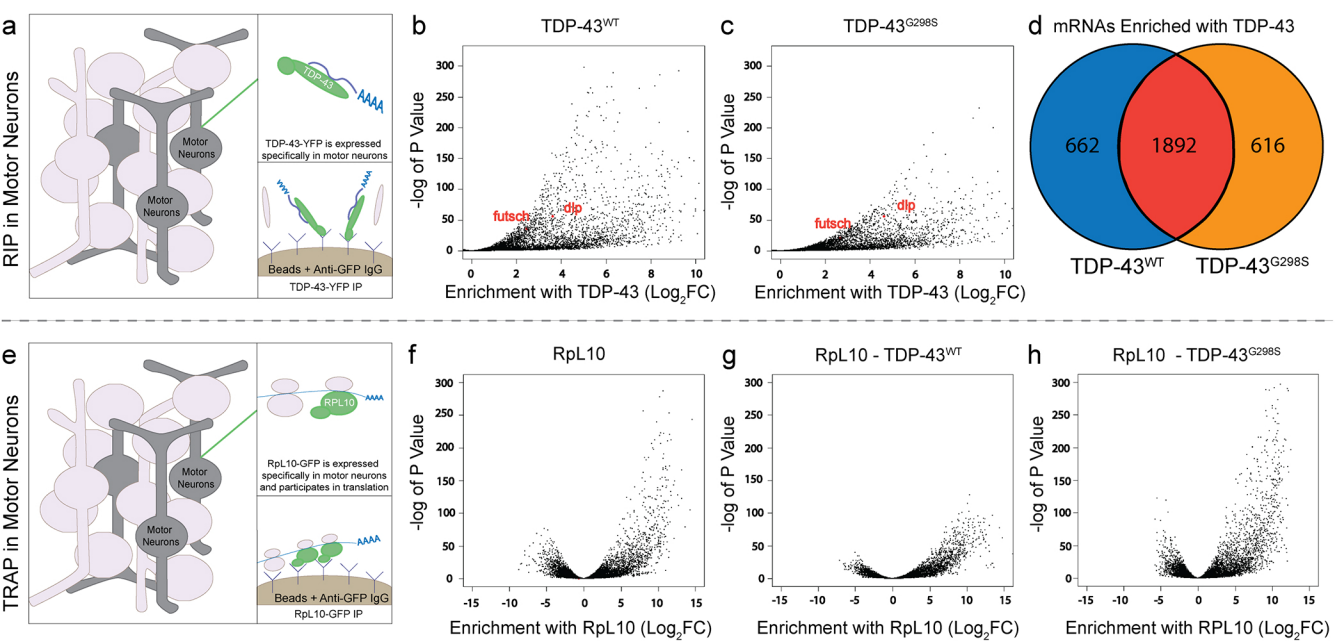
a
RIP in Motor Neurons
Motor Neurons
Motor Neurons
TDP-43
AAAA
TDP-43-YFP is expressed specifically in motor neurons
Beads + Anti-GFP IgG
TDP-43-YFP IP
b
TDP-43WT
-log of P Value
Enrichment with TDP-43 (Log2FC)
futsch
dlp
c
TDP-43G298S
-log of P Value
Enrichment with TDP-43 (Log2FC)
futsch
dlp
d
mRNAs Enriched with TDP-43
662
1892
616
TDP-43WT
TDP-43G298S
e
TRAP in Motor Neurons
Motor Neurons
Motor Neurons
RPL10
AAAA
RpL10-GFP is expressed specifically in motor neurons and participates in translation
Beads + Anti-GFP IgG
RpL10-GFP IP
f
RpL10
-log of P Value
Enrichment with RpL10 (Log2FC)
g
RpL10 - TDP-43WT
-log of P Value
Enrichment with RpL10 (Log2FC)
h
RpL10 - TDP-43G298S
-log of P Value
Enrichment with RPL10 (Log2FC)

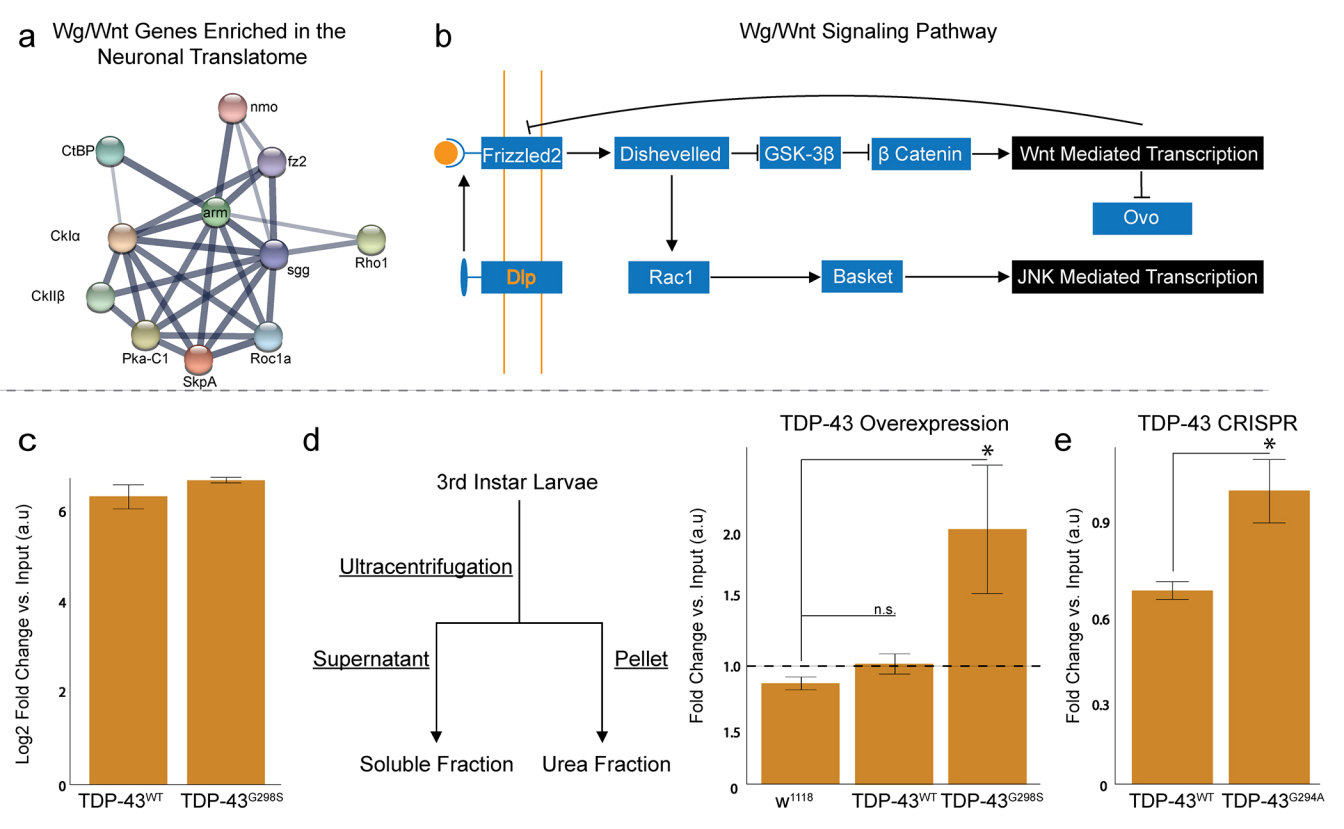
a
Wg/Wnt Genes Enriched in the Neuronal Translatome
nmo
CtBP
fz2
arm
Ckla
Rho1
sgg
CkIIβ
Pka-C1
Roc1a
SkpA
b
Wg/Wnt Signaling Pathway
Frizzled2
Dishevelled
GSK-3β
β Catenin
Wnt Mediated Transcription
Ovo
Dlp
Rac1
Basket
JNK Mediated Transcription
c
Log2 Fold Change vs. Input (a.u)
6
4
2
0
TDP-43WT
TDP-43G298S
d
3rd Instar Larvae
Ultracentrifugation
Supernatant
Pellet
Soluble Fraction
Urea Fraction
TDP-43 Overexpression
Fold Change vs. Input (a.u)
2.0
1.5
1.0
1.5
0
*
n.s.
w1118
TDP-43WT
TDP-43G298S
e
TDP-43 CRISPR
Fold Change vs. Input (a.u)
0.9
0.6
0.3
0
*
TDP-43WT
TDP-43G294A

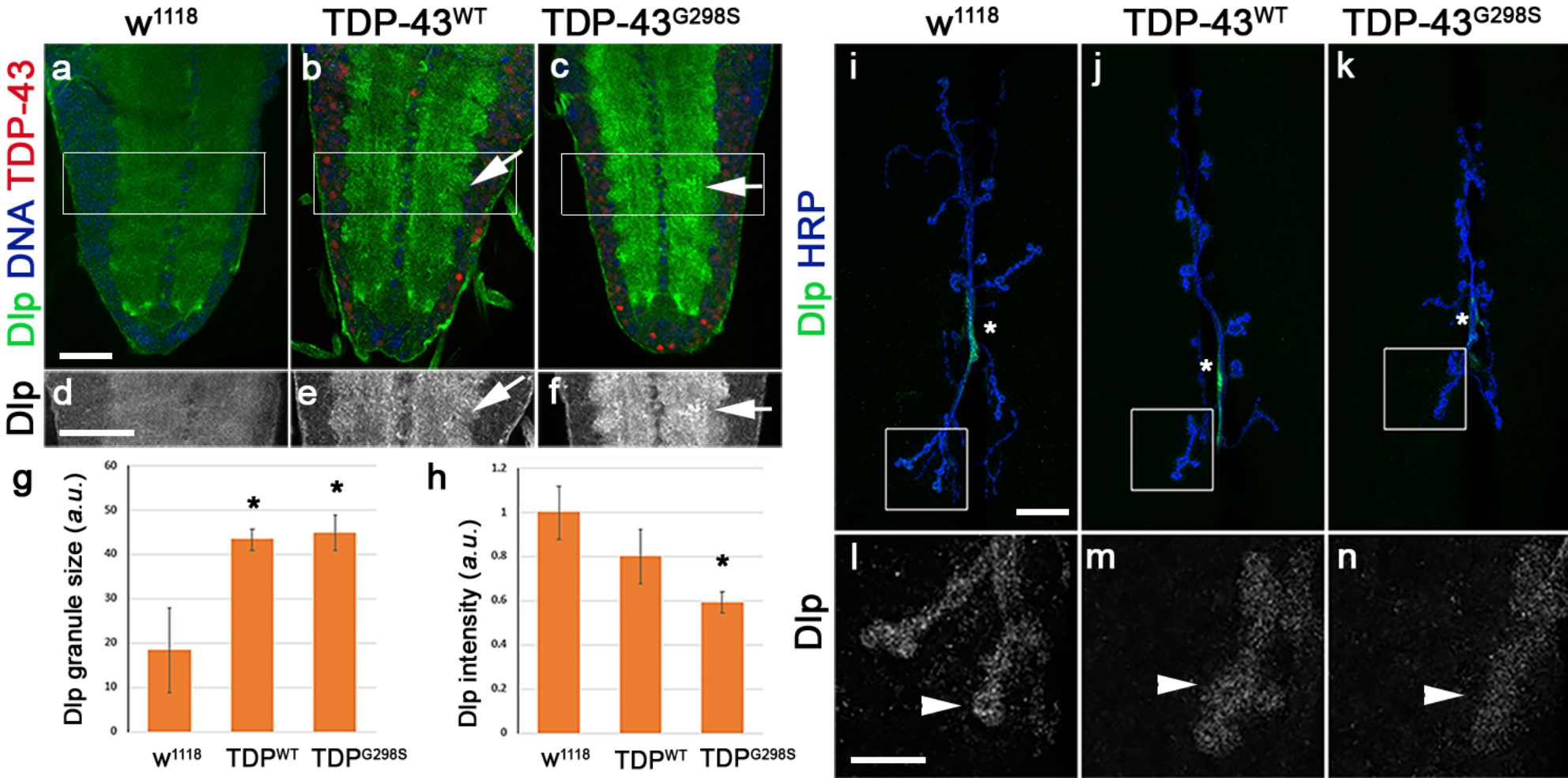
w1118
TDP-43WT
TDP-43G298S
Dlp DNA TDP-43
a
b
c
Dlp
d
e
f
g
Dlp granule size (a.u.)
60
50
40
30
20
10
0
*
*
w1118
TDPWT
TDPG298S
h
Dlp intensity (a.u.)
1.2
1
0.8
0.6
0.4
0.2
0
*
w1118
TDPWT
TDPG298S
w1118
TDP-43WT
TDP-43G298S
Dlp HRP
i
j
k
*
*
*
Dlp
l
m
n

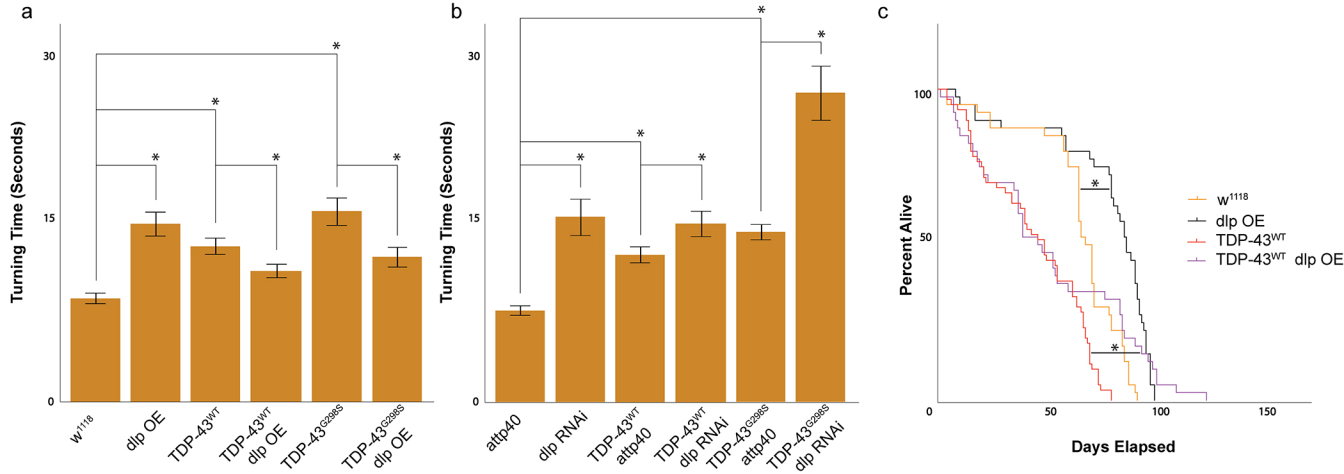
a
Turning Time (Seconds)
30
15
0
*
w1118
dlp OE
TDP-43WT
TDP-43WT dlp OE
TDP-43G298S
TDP-43G298S dlp OE
b
Turning Time (Seconds)
attp40
dlp RNAi
TDP-43WT attp40
TDP-43WT dlp RNAi
TDP-43G298S attp40
TDP-43G298S dlp RNAi
c
Percent Alive
100
50
0
50
100
150
Days Elapsed
w1118
dlp OE
TDP-43WT
TDP-43WT dlp OE

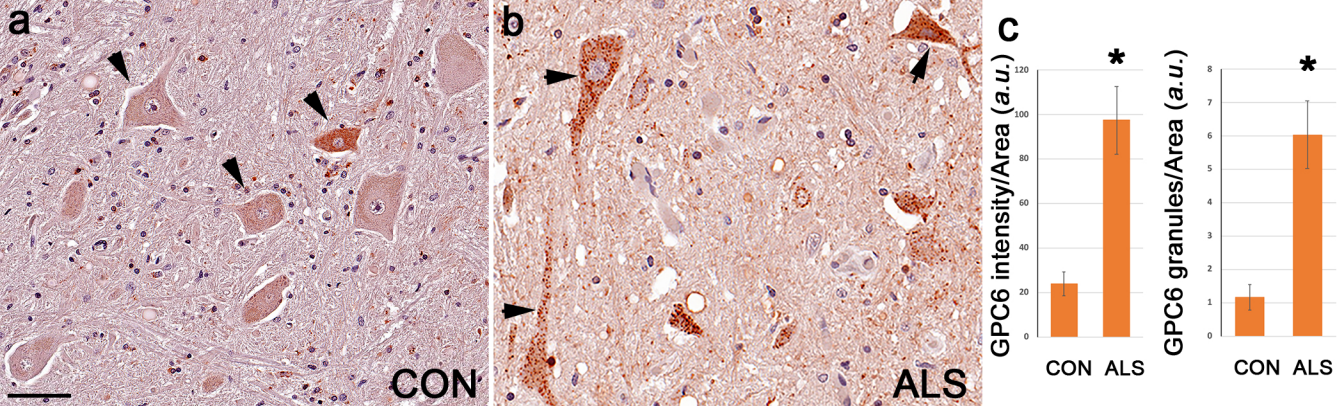
a
CON
b
ALS
c
GPC6 intensity/Area (a.u.)
120
100
80
60
40
20
0
*
CON
ALS
GPC6 granules/Area (a.u.)
8
7
6
5
4
3
2
1
0
*
CON
ALS

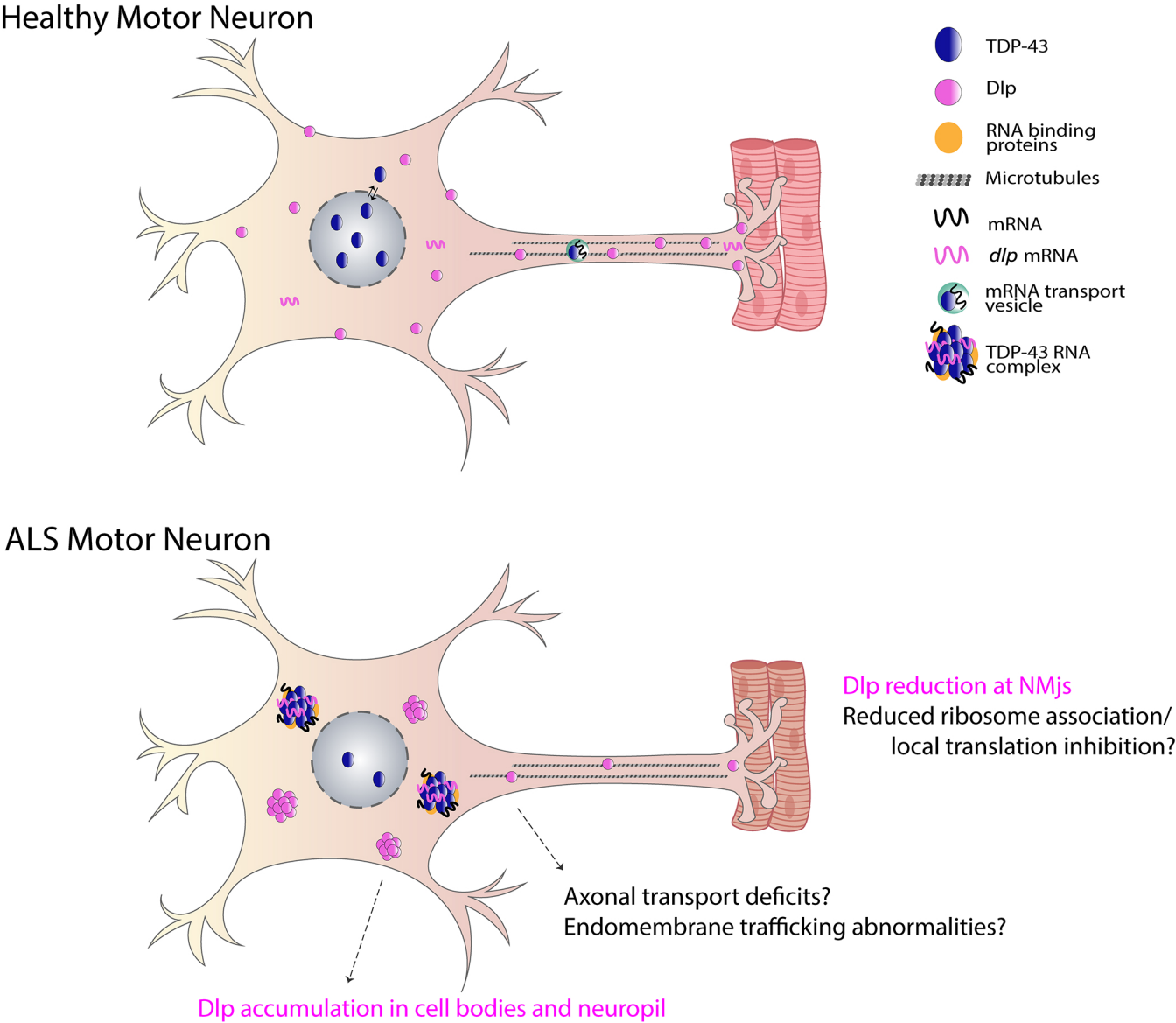
Healthy Motor Neuron
TDP-43
Dlp
RNA binding proteins
Microtubules
mRNA
dlp mRNA
mRNA transport vesicle
TDP-43 RNA complex
ALS Motor Neuron
Dlp reduction at NMjs
Reduced ribosome association/ local translation inhibition?
Axonal transport deficits?
Endomembrane trafficking abnormalities?
Dlp accumulation in cell bodies and neuropil

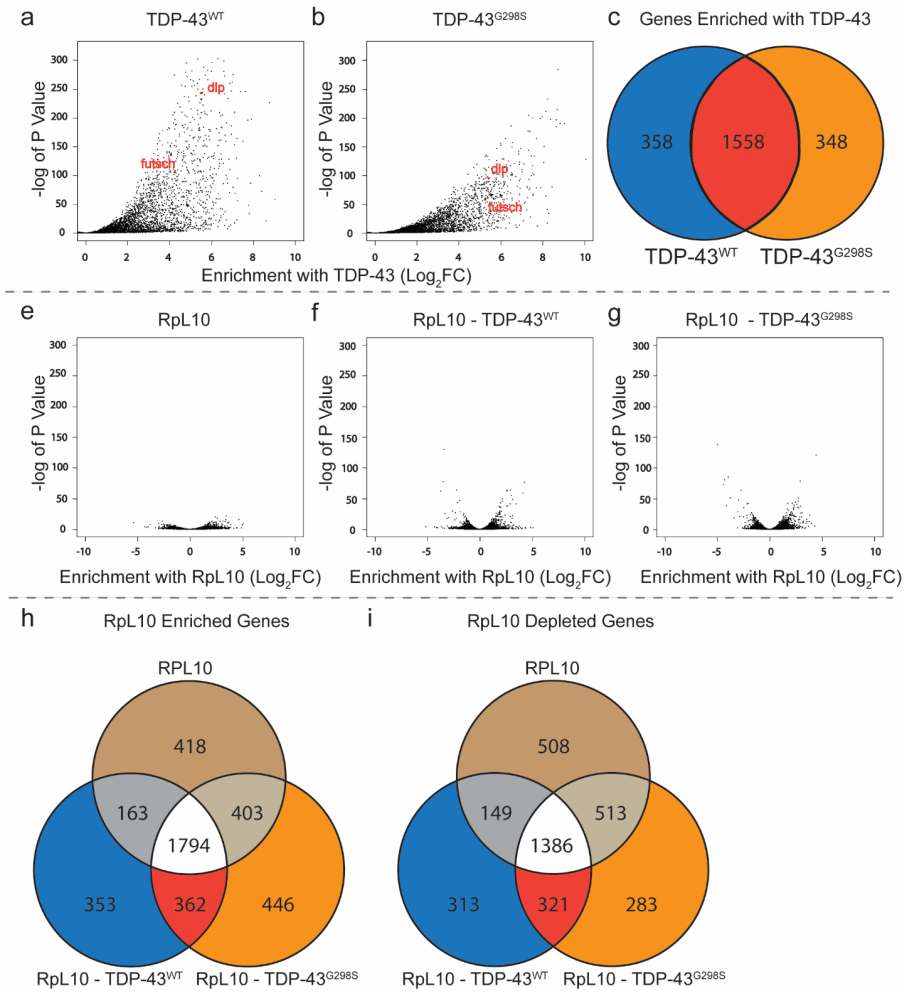

Figure S1. RIP and TRAP relative to Whole Larvae Inputs

(a,b). Volcano plot displaying RNAs enriched with TDP-43 during (a) TDP-43^{WT} and (b) TDP-43^{G298S} proteinopathy relative to transcript levels in whole ventral nerve cord. **(c).** Overlap between genes enriched with TDP-43 in two disease models (padj <0.05, log2foldchange > 1). **(e,f,g).** Volcano plots displaying RNA enrichment with RPL10 in (e) w^{1118} control 3rd instar larvae, (f) TDP-43^{WT} expressing larvae and (g) TDP-43^{G298S} expressing larvae relative to transcript levels in whole ventral nerve cords. **(h,i)** Overlap between genes enriched (h) or depleted (i) with RpL10 in two disease models (padj <0.05, log2foldchange > 1).

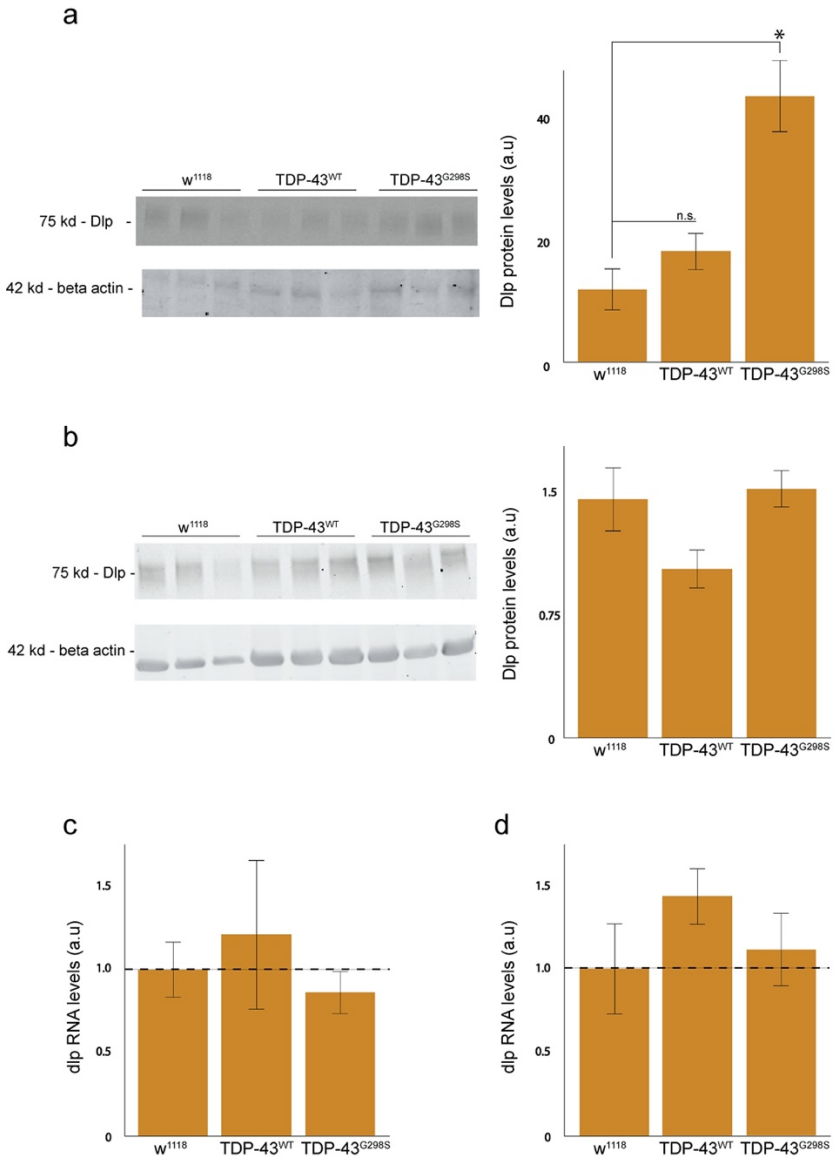

Figure S3. Alterations to *dlp* RNA levels were not detected in either the NMJ or the whole VNC (a). Western blot assaying Dlp protein and beta actin in dissected VNCs. **(b).** Western blot assaying Dlp protein and beta actin in dissected neuromuscular junctions. **(c).** Quantification of *dlp* mRNA relative to *GPDH* in dissected VNCs. N = 3. Significance determined through the Kruskall-Wallis test. **(d).** Quantification of *dlp* mRNA relative to *GPDH* in dissected NMJs. N = 3. Significance determined through the Kruskall-Wallis test. * = $P_{value} < 0.05$.